Dynamic spectrum of long wave terrestrial radio signals during episodes of ionospheric disturbances caused by solar activity

Shaik Manoj, Shanmugha Sundaram G.A*

Electronics and Communication Engineering, Amrita Vishwa Vidyapeetham, Coimbatore, India.

*Corresponding author: E-Mail: Shaikmanoj123@gmail.com

ABSTRACT

The dynamic spectral record of long wave radio signals (kHz band) had registered a disturbed condition of the ionosphere region involved with propagation of these signals. The reason for such signatures in the dynamic spectrogram can be accredited to the impact of Solar Energetic Particles (SEP) on the ionosphere along the propagation path of terrestrial long wave radiation, studied using the Multi-Hop propagation model. Points of reflection in the ionosphere directly above specific locations above the earth where determined. Total Electron Content (TEC) values for such regions were obtained from interputing the Global Positioning System (GPS) data. From a comparison of such results during periods when the Sun was quiet and active periods, the magnitude of ionosphere disturbance contributed by the various active solar phenomena's has been determined. The paper is based on the impact of Geomagnetic storm (Kp=6) on the TEC, that occurred on 16 April 2015. Long wave radio signals from transmitters located in places like United States Navy near Lualualei, Hawaii (Geomagnetic lat 21°25′13.38″N, Geomagnetic long 158°09′14.35″W) and Rosnay near France (Geomagnetic lat 46°42'47"N, Geomagnetic long 1°14'39"E) were monitored closely to know extent of the impact.

KEY WORDS: Antennas, Electromagnetic radiation, Global Positioning System, Ionosphere, Radio frequency.

1. INTRODUCTION

Geomagnetic storm is one the fascinating event ever since ancient times. It is used intensively for calibrating different physical hypotheses by the scientists. The atmospheric effects of a geomagnetic storm are primarily subjected on Ionospheric parameters. In spite of numerous studies relating to geomagnetic storms, the occurrence is always different under different situations. Geomagnetic storm is one of significant proceedings for ionospheric study since it has a direct effect on the Earth's ionosphere. Geomagnetic storms are the significant disturbances that influence the Magnetosphere happen when the interplanetary attractive field turns southward and stays southward for a delayed Period of time. During a geomagnetic storm's distinct period, which can keep going the length of two to more than two days on account of an extreme storm charged particles in the close Earth plasma sheet are empowered and injected deeper into the inner magnetosphere, producing the storm-time ring current. This stage is described by the event of various serious sub storms, with the accompanying auroras and geomagnetic impacts. At the point when the interplanetary field turns northward.

2. MATERIALS AND METHODS

Ionosphere: The ionosphere is an area of the upper atmosphere in which the thickness of free electrons is sufficiently substantial to have an obvious impact on the propagation of radio waves. Although boundaries of the ionosphere both lower and upper are not well defined, for most of the practical purposes they can be considered to occur roughly around 50km and 1000km. The ionosphere is formed by the ionising impacts of solar X-rays and ultraviolet radiations on the neutral gasses in the upper atmosphere. Together, these two impacts lead to the formation of a region of maximum electron density, known as a Chapman layer, at altitudes around 250km and Maintaining the Integrity of the Specifications.

Total Electron Content (TEC): The calculation of Total Electron Content (TEC) of the ionosphere evolve into very essential in modern periods, in context of the growing need for the transionospheric communications which is utilized in the space-borne navigating vehicles. TEC is characterized as number of total electrons incorporated along the way from each GPS to the receiver. TEC as a pointer of ionospheric unpredictability is determined by the reformed GPS signal through number of available electrons. Where, 1 Total Electron Content unit =1016electrons/meters².

Long Wave Terrestrial Radio Signals: Longwave signals are generally of long wavelengths that are mentioned in radio spectrum – usually in kilometer-sized or greater. The most widely recognized description is the wavelength of the radio band more than 1000mts(frequencies under 300 kHz) [6,7,8] incorporating the very low frequency (VLF) (3–30 kHz) bands and low frequency (LF) (30–300 kHz), at times some piece of the medium frequency (MF) band (300–3000 kHz) ITUs are incorporated. Very low frequency or VLF is the ITU designation for radio frequencies (RF) in the wavelengths from 10 to 100 kilometers and can vary between 3 kHz to 30 kHz.

Table.1. Specific VLF Transmitters details

Call sign	Frequency(khz)	Location	Latitude	Longitude
NPM	21.400	Lualuahei, Hawaii	N 21^0 25' 13.38"	W 158^0 09'14.35"
HWU	22.600	Rosnay, France	N 46^0 42' 47.26"	W 001^0 14'42.89"

Global Positioning System: GPS is a satellite based radio navigation system that gives precise position, time and velocity information globally and persistently under all weather conditions. Despite the fact that GPS is owned and operated by the US Department of Defense (DOD) and was developed primarily for defence operations, it is currently utilized widely in both the defense and civilian communities in most of the countries. A simple way of describing the GPS system is to divide it into the following three fragments:

•   The Space Segment
•   The Control Segment, and
•   The User Segment (the GPS receivers).

        The Space Segment comprises of 24 GPS satellites which are arranged in 6 orbital planes each of which are inclined at 550 to the equator. The Control Segment comprises of four ground antennas and four monitor stations which are distributed all around the Earth, and a master control station located in Colorado Springs. The User Segment comprises of GPS receivers, both civilian and military, and the related infrastructure such as differential stations.

Dates: Solar activity was significantly low neglecting few disturbances in between, But during the 2nd and 3rd weeks of April 2015 significant disturbances were observed due to a Geomagnetic storm (Kp>6), especially on April 16th 2015, and observations were noted down with the help of Square Loop Antenna and Spectrum Lab software.

Location: In this work we monitored and observed the impact of geomagnetic storm on NPM Transmitter Lualualei, Hawaii and VLF Rosnay HWU Transmitter, France.

NPM Transmitter Lualualei: A very-low-frequency (VLF) transmitting antenna has been built for the United States Navy at the Naval Transmitting office (call sign NPM), Lualualei. As a piece of the Proof of Performance assessment of the new antenna, faculty from the Naval Research laboratory (IRL) resolute the antenna system radiation ranges along with radiation resistance, radiated power and effective pitch, in November and December 1971. As well as the antenna system was certified for likely corona circumstances. This transmitter has radiated power of ~500KW operating at a frequency of 21.4 KHz.

| **Figure.1.VLF transmitter Lualualei, Mast** | **Figure.2.HWU transmitter France** | **Figure.3.Square Loop Antenna** |

VLF Rosnay Transmitter (HWU): HWU transmitter is a French feature for broadcasting the directions to the afloat submarines of the French Navy. Rosnay transmitter which is stationed close to Rosnay is one of the sky scraping transmitters located at France and it is evidently seen from the satellite images. It utilizes an antenna supported by 13 guyed masts. HWU transmitter works on 22.6 KHz frequency and the transmitter has radiated power of ~400KW.

Square Loop Antenna: A square loop antenna has 0.762m sides. It has PVC cross-beam and has 25 turns of insulated magnet wire. Antenna is made to stand upright by building a feet on base. This will give support to the loop antenna.

Spectrum Lab: Spectrum lab is mainly used to measure the peak frequencies and amplitude of signals. This peak detecting mode provides sub MilliHertz accuracy after calibration. The spectrum lab is a program which analyzes the spectrum of audio signal PC soundcard. The audio signal is recorded as .wav file and it can be further used for analysis. It also performs the nth order audio filtering in real time and the output is send to soundcard. The data is plotted which is calculated by signal analysis function. Transmit and receive the audio streams with timestamp from GPS receiver over internet. The window may look like figure 4,

Table.2.Characteristics OF Loop Antenna

Parameter	Value	Parameter	Value
Wire	17 AWG	Square frames	1m
Length Dimension	120m	Inductance	4.65mH
Turns	25		

TEC Equation:

The group delay can be derived as

$$P_1 - P_2 = 40.3 TEC \left(\frac{1}{f_2^2} - \frac{1}{f_1^2} \right) \qquad (1)$$

Total Electron Content can be given as

$$TEC = \frac{1}{40.3} \left(\frac{f_1 f_2}{f_1 - f_2} \right) (P_2 - P_1) \qquad (2)$$
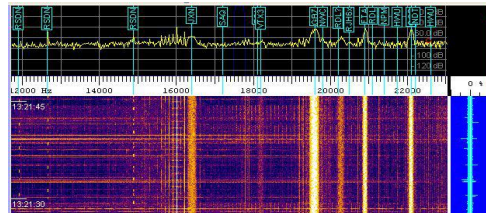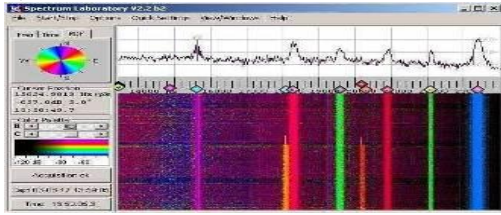
www.jchps.com
ISSN: 0974-2115
Journal of Chemical and Pharmaceutical Sciences

Figure.4. a)Spectrum Lab main window; (b)VLF spectrum/spectrogram with 'Radio Station' display

Modeling of Radio path Hop:

T_x = location of the transmitter over the Earth's surface
β = antenna take off angle
90-γ = angle of incidence in the ionosphere
I = point of reflection in the ionosphere
d = distance of the point of reflection from the transmitter
H = altitude of the layer of the ionosphere where reflection occurs
P = projection of the point of reflection over the Earth's surface
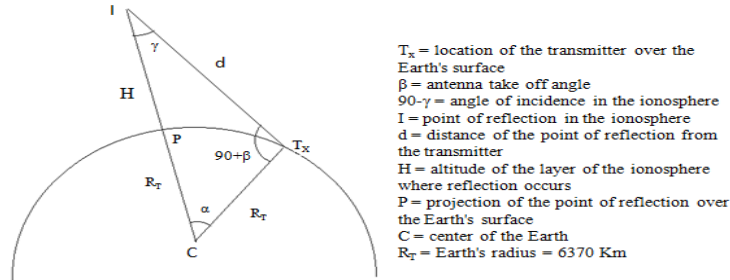C = center of the Earth
R_T = Earth's radius = 6370 Km

Figure.5.Geometry of the Ionospheric hop

In order to find out the geometry of an ionospheric radio link, we analyse the geometry for one hop and generalize the outcomes. The figure 5 will be handy for the analysis,

Extent of the radio path: In order to calculate d, we make use of triangle shaped from the points T_x-I-C and cosine laws.

$$(R_T + H)^2 = d^2 + R_T^2 + 2dR_T\cos(90 + \beta) \quad (3)$$

If we evaluate the term on the left side of (3), we can get the following quadratic equation (4), being d undefined,

$$d^2 + 2dR_T\cos(90 + \beta) - H(H + 2R_T) = 0 \quad (4)$$

Hop Distance: To compute this Hop's distance, it is essential to know the value of the angle alpha (which is in degrees), alpha can be computed by means of law of sines for the triangle T_x-I

$$\sin(\propto) = \frac{d\sin(90+\beta)}{R_T+H} \Longrightarrow \alpha = \left[\frac{d\sin(90+\beta)}{R_T+H}\right] \quad (5)$$

Now d_A can be measured as,

$$d_A = \frac{2\pi R_T\alpha}{360} = \frac{2\pi(6370\times10.08)}{360} = 1120.668931\ K_m \quad (6)$$

Where the distance d among the points T_x and I was   measured using (6), consequences hop distance is given as,

$$d_{HOP} = 2d_A = \frac{4\pi R_T \arcsin\left[\dfrac{d\sin(90+\beta)}{R_T+H}\right]}{360} \quad (7)$$

$$d_{Hop} = 2241.337863\ \text{Km}$$

In this study two vlf stations were taken as mentioned above Lualualei VLF transmitter in Hawaii and HWU transmitter at Rosnay in France(HWU) and their modeled paths and number of hops to reach Receiver (Rx) were shown in the figures 6 and 7 respectively,

Figure.6.Number of Hops that Signal Experienced on its way to the receiver from NPM Transmitter

Figure.7.Number of Hops that Signal Experienced on its way to the receiver from HWU Transmitter

3. RESULTS AND DISCUSSIONS

Table.3.VLF stations along with the ionospheric plasma frequency disturbance

Date	VLF Station		Spectrum Lab Data Time (UT)		Ionospheric Plasma Frequency (kHz)	
	Call Sign	Frequency (kHz)	Start	End	Start	End
9th April, 2015.	VTX2	17.00	20:20	20:24	No Change	
	GBZ	19.58	20:23	20:25	19.57	19.68
	NWC	19.80	20:30	20:32	No Change	
	NPM	**21.40**	**20:21**	**20:25**	**21.39**	**21.53**
	NDT	22.20	20:25	20:27	22.18	22.26
	HWU	**22.60**	**20:27**	**20:39**	**22.58**	**22.70**
	DH038	23.40	20:28	20:30	No Change	
10th April, 2015.	VTX2	17.00	06:25	06:28	No Change	
	GBZ	19.58	06:27	06:29	19.56	19.59
	NWC	19.80	04:54	04:56	No Change	
	NPM	**21.40**	**07:11**	**07:15**	**21.38**	**21.48**
	NDT	22.200	06:48	06:50	22.18	22.26
	HWU	**22.60**	**07:06**	**07:09**	**22.50**	**22.68**
	DH038	23.40	07:04	07:06	No Change	
11th April, 2015.	VTX2	17.00	14:38	14:42	No Change	
	GBZ	19.58	14:44	14:46	19.57	19.60
	NWC	19.80	14:46	14:49	No Change	
	NPM	**21.40**	**14:50**	**14:53**	**21.21**	**21.58**
	NDT	22.20	17:17	17:19	22.17	22.26
	HWU	**22.60**	**14:42**	**14:46**	**22.48**	**22.99**
	DH038	23.40	14:45	14:47	No Change	
12th April, 2015	VTX2	17.00	16:29	16:31	No Change	
	GBZ	19.580	16:38	16:41	19.57	19.59
	NWC	19.80	17:22	17:25	No Change	
	NPM	**21.40**	**17:36**	**17:39**	**21.38**	**21.43**
	NDT	22.20	21:00	21:03	21.15	22.28
	HWU	**22.60**	**21:06**	**21:09**	**22.56**	**22.68**
	DH038	23.40	22:02	22:04	No Change	
13th April, 2015	VTX2	17.00	00:43	00:47	No Change	
	GBZ	19.58	03:15	03:18	19.57	19.68
	NWC	19.80	03:31	03:32	No Change	
	NPM	**21.40**	**03:19**	**03:25**	**21.29**	**21.63**
	NDT	22.20	16:27	16:29	21.19	22.22
	HWU	**22.60**	**16:32**	**16:34**	**22.59**	**23.10**
	DH038	23.40	03:32	03:35	No Change	
14th April, 2015	VTX2	17.00	06:36	06:39	No Change	
	GBZ	19.58	04:42	04:45	19.57	19.60
	NWC	19.80	08:41	08:43	No Change	
	NPM	**21.40**	**08:46**	**08:52**	**21.20**	**21.80**
	NDT	22.20	09:31	09:33	22.15	22.25
	HWU	**22.60**	**08:58**	**09:02**	**22.50**	**22.99**
	DH038	23.40	10:00	10:02	No Change	
15th April, 2015	VTX2	17.00	03:13	03:13	No Change	
	GBZ	19.58	03:29	03:29	19.56	19.68
	NWC	19.80	04:22	04:22	No Change	
	NPM	**21.40**	**03:28**	**03:28**	**21.38**	**21.54**
	NDT	22.20	06:22	06:22	21.19	22.21
	HWU	**22.60**	**03:30**	**03:30**	**22.58**	**22.62**
	DH038	23.40	07:20	07:20	No Change	
16th April, 2015	VTX2	17.00	03:32	03:34	No Change	
	GBZ	19.58	03:39	03:41	19.55	19.61
	NWC	19.80	04:02	04:03	No Change	
	NPM	**21.40**	**03:36**	**04:48**	**21.20**	**21.98**
	NDT	22.20	04:11	04:15	21.19	22.27
	HWU	**22.60**	**03:31**	**04:45**	**22.38**	**23.21**
	DH038	23.40	05:12	05:14	No Change	

In Table 3, VLF stations with Spectrum Lab and Ionospheric Plasma Frequency (kHz) Disturbances along with the Date and Time (UT) was clearly tabled. In this work we mainly concentrated on NPM and HWU VLF stations were Maximum disturbances were felt due to strong Solar Activity On 16th April 2015 (between 3:28-4:49 UT).

Table.4.Sunspot Region 2322 summary

Date	Location		Sunspot Characteristics				
	Lat CMD	Helio Lon	Area 10-6 hemi	Extent (helio)	Spot Class	Spot Count	Mag Class
13Apr, 2015	N14E12	123	30	5	Dao	4	B
14Apr, 2015	N1W02	124	20	5	Bxo	3	B
15Apr, 2015	N1W13	121	10	5	Bxo	3	B
16Apr, 2015	**N1W25**	**120**	**10**	**5**	**Bxo**	**2**	**B**
17Apr, 2015	N1W39	121	40	6	Dai	3	B
18Apr, 2015	N1W 50	118	10	2	Hrx	2	A
19Apr, 2015	N1W62	118	10	4	Bxo	3	B

Table.5.Solar Flares List

Date	Time (UT)			Optical			
	Begin	Max	End	X-ray class	Imp/Brtns	Location LatCMD	Rgn #
13Apr, 2015	08:21	08:26	08:28	C4.7	SF	N15E26	2322
14Apr, 2015	22:35	22:35	22:46	-	SF	N11E41	2321
15Apr, 2015	11:35	11:42	11:53	C1.5	SF	N14E22	2321
16Apr, 2015	**09:00**	**09:07**	**09:14**	**C5.7**	**1F**	**N25E48**	**2324**
17Apr, 2015	09:27	09:32	09:39	C1.1	SF	N08E43	2325
18Apr, 2015	18:09	18:25	18:38	C2.9	1F	N11W22	2321
19Apr, 2015	06:40	07:19	07:45	C2.2	1F	N10W58	2322

In Table 4 and 5 Sun Spot Region 2322 and Solar flare day to day activity was closely monitored and tabled from 13th April to 19th April, 2015. In this work we focused on NPM Transmitter Lualualei, Hawaii and HWU transmitter in French during 16th April where strong disturbances were seen on these two stations due Geomagnetic storm(K_p=6) and a Solar flare of class C 5.6.

Spectrum Lab Observations: On April 16th 2015 from 4:02 to 4:23 UT (hours) clear disturbance was registered from both vlf transmitters NPM (21.4 kHz) and HWU (22.6 kHz) due to Geomagnetic storm (K_p=6) and C 5.7 solar flare. Strong Temperal and spectral changes were seen along with intense intensity, along with these loosing of singal information for every possible 2 secs was recorded which is clearly shown in the figure 8. Along with the above mentioned disturbances there were disturbances seen like Doted lines, zig zag motion of the signal and change in the intensity and bright ness levels etc.
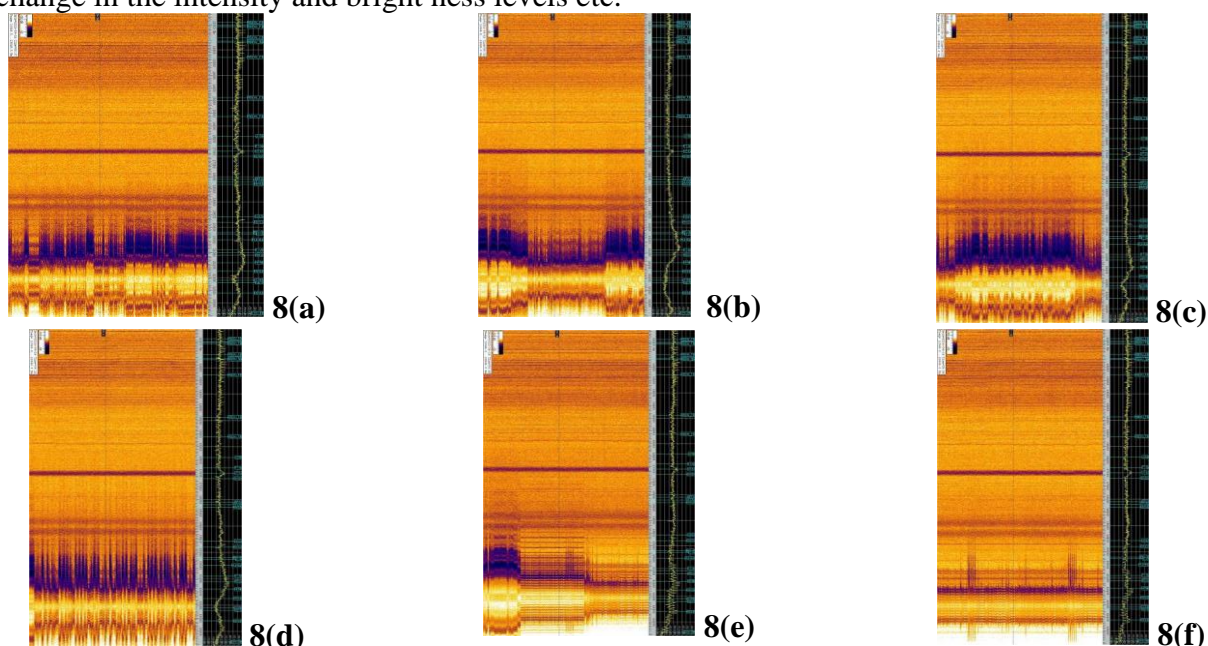

Figure.8.Disturbance due to Geomagnetic storm Seen During 16th April 2015 for NPM and HWU Stations were ploted using Spectrum Lab

Using GPS_TEC for TEC analysis: In this paper we concentrated on Geomagnetic Storm and solar flares to estimate TEC changes during the flare, Geomagnetic storm periods and consider diurnal variations on TEC change compared with X-Ray flux which we obtain from GOES 15 X- Ray Flux plots and with GPS_TEC software which is created by Dr. Gopi Krishna Seemala. For this we considered two vlf stations one is Thailand and other is Macedonia during the Geomagnetic storms active and quite periods were plotted. The process for Macedonia and Thailand were illustrated in Figures 9 and 10 respectively. Redline–Average (2 sigma iterated) TEC over all PRNs (output file: *.std) and Green line–vertical TEC from individual PRNs, here datapresented is above 20 deg elevation angles (output file: *.cmn, it contains all eleva-tionangles).
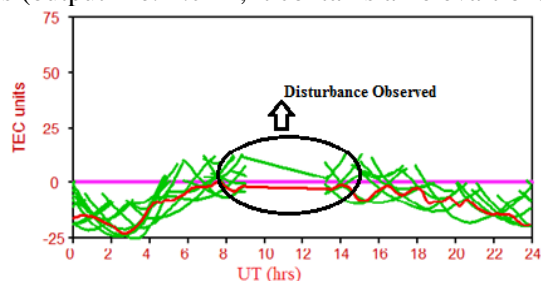

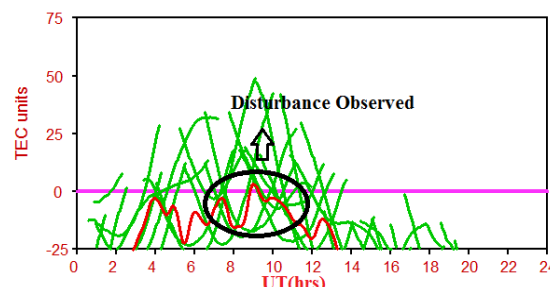**Fig.9.TEC plots for Macdonia on 16ᵗʰ April 2015(ORID)**

Fig.10.TEC plots for Thailand on 16ᵗʰ April 2015(CUSV)

To estimate the impact of the Geomagnetic storm and C 5.7 solar flare on the NPM and HWU Transmitters on 16ᵗʰ April, we modeled a radio path for the signals from the Transmitter (T_x) to the Receiver (R_x). In case of NPM transmitter the radio signal passed through places like Macedonia, Syria, Iraq, Iran and finally to the receiver at Coimbatore. For the further analysis we took the GPS data (RINEX) from the GPS stations located at Macdonia (ORID) and Thailand (CUSV) on 16ᵗʰ April 2015, and were pocessed by GPS_TEC software and clear disturbance was seeen due to solar activity, and clear disturbances were seen in regarding Electron Flux, Photon Flux, GOES H_p and Estimated K_p (data obtained from Space Weather Prediction Center (SWPC)).

4. CONCLUSION

In this work we monitored the effects of geomagnetic storm and solar flare on the lower ionosphere. It is seen geomagnetic storm especially causing considerable electron density changes, causing phase perturbations and significant amplitude changes. Consequences indicate the magnitude of the disturbed signals exactly correlated to the power intensity of the consequent events occurred. More over studies exposed disturbed vlf signals from both Hawaii (NPM), Rosnay (HWU) stations were observed due to the powerful geomagnetic storm, acquire longer recuperation periods when assessed with the other signal at that time.

REFERENCES

Davies K, Ionospheric Radio, vol.31, IEE Electromagnetic Waves Series, Peter Peregrinus Ltd., 1990.

Fejer, Bela G, and Ludger Scherliess, Time dependent response of equatorial ionospheric electric fields to magnetospheric disturbances, Geophysical Research Letters, 22 (7), 1995, 851-854.

Guha, Anirban, Response of the equatorial lower ionosphere to the total solar eclipse of 22 July 2009 during sunrise transition period studied using VLF signal, Journal of Geophysical Research: Space Physics (1978–2012).

Guyer S, and Can Z, Solar flare effects on the ionosphere, Recent Advances in Space Technologies (RAST), 2013 6th International Conference on IEEE, 2013.

Kelley, Michael C, Penetration of the solar wind electric field into the magnetosphere/ionosphere system, Geophysical Research Letters, 30 (4), 2003.

Kumar, Sanjay, and Singh A.K, The effect of geomagnetic storm on GPS derived total electron content (TEC) at Varanasi, India, Journal of Physics: Conference Series, IOP Publishing, 208 (1), 2010.

Rishbeth H, Basic physics of the ionosphere: a tutorial review, Journal of the Institution of Electronic and Radio Engineers, 58.6S, 1988, S207-S223.

Yaacob, Norsuzila, Mahamod Ismail, and Mardina Abdullah, GPS total electron content (TEC) prediction at ionosphere layer over the Equatorial region, INTECH Open Access Publisher, 2010.